

Chromatography at $-30\text{ }^{\circ}\text{C}$ for Reduced Back-Exchange, Reduced Carryover, and Improved Dynamic Range for Hydrogen–Deuterium Exchange Mass Spectrometry

Kyle W. Anderson and Jeffrey W. Hudgens*


 Cite This: *J. Am. Soc. Mass Spectrom.* 2022, 33, 1282–1292


Read Online

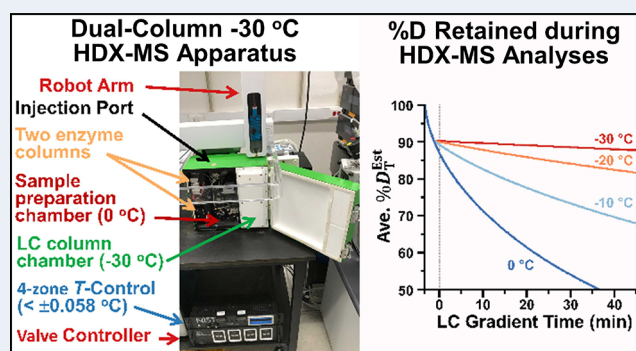
ACCESS |

 Metrics & More

 Article Recommendations

 Supporting Information

ABSTRACT: For hydrogen–deuterium exchange mass spectrometry (HDX-MS) to have an increased role in quality control of biopharmaceuticals, H for D back-exchange occurring during protein analyses should be minimized to promote greater reproducibility. Standard HDX-MS analysis systems that digest proteins and separate peptides at pH 2.7 and $0\text{ }^{\circ}\text{C}$ can lose $>30\%$ of the deuterium marker within 15 min of sample injection. This report describes the architecture and performance of a dual-enzyme, HDX-MS instrument that conducts liquid chromatography (LC) separations at subzero temperature, thereby reducing back-exchange and supporting longer LC separations with improved chromatographic resolution. LC separations of perdeuterated, fully reduced, iodoacetamide-treated BSA protein digest standard peptides were performed at 0 , -10 , -20 , and $-30\text{ }^{\circ}\text{C}$ in ethylene glycol (EG)/ H_2O mixtures. Analyses conducted at -20 and $-30\text{ }^{\circ}\text{C}$ produced similar results. After subtracting for deuterium retained in arginine side chains, the average peptide eluted during a 40 min gradient contained $\approx 16\%$ more deuterium than peptides eluted with a conventional 8 min gradient at $0\text{ }^{\circ}\text{C}$. A subset of peptides exhibited $\approx 26\%$ more deuterium. Although chromatographic peaks shift with EG concentration and temperature, the apparatus elutes unbroadened LC peaks. Electrospray ion intensity does not decline with increasing EG fraction. To minimize bias from sample carryover, the fluidic circuits allow flush and backflush cleaning of all enzyme and LC columns. The system can perform LC separations and clean enzyme columns simultaneously. Temperature zones are controlled $\pm 0.058\text{ }^{\circ}\text{C}$. The potential of increased sensitivity by mixing acetonitrile with the analytical column effluent was also examined.



INTRODUCTION

Hydrogen–deuterium exchange mass spectrometry (HDX-MS) is a powerful tool for investigating protein dynamics, including protein–ligand interactions, folding dynamics, and interactions among proteins including antibodies, glycoproteins, lipoproteins, membrane proteins, virus fragments, enzymes, chaperones, amyloids, fibrils, and pharmaceuticals.^{1–3} In the biopharmaceutical discovery and development sector HDX-MS data have been used to substantiate and protect intellectual property and to evaluate physicochemical similarity between a biosimilar candidate and the originator product.^{4,5} In addition, HDX-MS data are increasingly provided to support biologics license applications (BLAs).⁶

The bottom-up HDX-MS measurement involves immersion of protein in D_2O for a specific labeling time t_{HDX} , proteolysis of the protein into peptides, liquid chromatographic (LC) separation of the peptides, mass spectrometric measurement of the isotopic envelope for each eluting peptide, and computation of peptide deuterium content, $D_{\text{Uncorrected}}^{\text{Peptide}}(t_{\text{HDX}})$ from the mass envelope. Back-exchange of H for D during the analysis process reduces the apparent peptide deuterium

content, and either short-term or long-term variations in back-exchange limit the reproducibility of the HDX-MS measurement. Back-exchange rates vary with residue and sequence. Reports of back-exchange in peptides range from 15% to 60%.^{7–18} Back-exchange is minimized by conducting analyses under cold, acidic conditions ($\approx \text{pH } 2.7$, $\approx 0\text{ }^{\circ}\text{C}$) and by limiting chromatographic gradients to short duration (6.0–9.5 min).^{19–21} Short gradients chosen to reduce back-exchange may not provide optimal separation of eluting peptides.

Because commercial lifecycles of biopharmaceutical products can span decades, the emergent application of HDX-MS for pharmaceutical quality control (QC) will require minimization of measurement drift. Applications that determine the comparability of biosimilars will also require quantitative

Received: March 31, 2022

Revised: June 8, 2022

Accepted: June 9, 2022

Published: June 22, 2022



HDX-MS of similar precision.^{5,22–31} HDX-MS measurement drift can be partially alleviated by reporting $D_{\text{Corrected}}^{\text{Peptide}}(t_{\text{HDX}})$'s that are corrected for H/D back-exchange and scaled to immersions in 100% D₂O.

Most commonly, $D_{\text{Corrected}}^{\text{Peptide}}(t_{\text{HDX}})$ is computed by an approximate formula given by Zhang and Smith that uses the centroid, $\langle m(t_{\text{HDX}} = \infty) \rangle^{\text{Peptide}}$, found for the perdeuterated protein.^{21,32,33} Each experimentally determined $\langle m(t_{\text{HDX}} = \infty) \rangle^{\text{Peptide}}$ captures all factors affecting back-exchange, including perturbations induced by peptide interactions with stationary phases,³⁴ peptide refolding, exchange acceleration by certain acids in the mobile phase,^{35,36} catalysis by histidine side chains in amides beyond nearest neighbors, and polymer end-chain effects.^{37,38}

We note that preparations of perdeuterated reference protein samples have occasionally proven impracticable.^{21,39} In these cases, the back-exchange correction provided by $\langle m(t_{\text{HDX}} = \infty) \rangle^{\text{Peptide}}$ is estimated by incorporating residue-specific back-exchange rates into a nonlinear fit of peptide data and by imposing appropriate boundaries for HDX rates.^{13,40–43} However, the veracity of computed corrections can suffer from difficulties associated with accurately simulating all the aforementioned exchange rate perturbations. Regardless, the uncertainty of each $D_{\text{Corrected}}^{\text{Peptide}}(t_{\text{HDX}})$ is decreased as total back-exchange is decreased. Accordingly, an operationally stable metrology platform that minimizes uncertainties associated with computation of $D_{\text{Corrected}}^{\text{Peptide}}(t_{\text{HDX}})$'s will improve comparability of HDX-MS data.

Over the past decade, several groups have introduced methods for suppressing back-exchange in top-down or bottom-up HDX-MS strategies. Amon et al. reported a top-down method that quenched and cooled protein samples to -15 °C, volatilized peptide ions from a chip-based nanoelectrospray source, and fragmented ions in an electron transfer dissociation (ETD) facility.⁴⁴ Similarly, Pan et al. demonstrated a top-down approach involving injection of a thawed, deuterium-labeled protein sample into a LC column at -20 °C that eluted sample into a mass spectrometer equipped with an ETD facility.^{45,46}

Several groups have reported strategies for suppressing back-exchange during bottom-up HDX-MS analyses by employing chromatography in aprotic solvents,¹⁵ supercritical fluids,¹⁰ and subzero temperature environments.^{47–50} Venable et al. investigated the use of several buffer modifiers (ethylene glycol (EG), dimethylformamide, methanol, and formamide) that depressed the solution freezing points to as low as -30 °C.⁴⁷ Using methanol as the buffer modifier, Wales et al. reported LC separations at -20 °C.⁴⁸ Zhang et al. conducted HDX-MS analyses of epitopes of birch pollen allergen at -9 °C by adding 4.5% ACN to mobile phase A.⁴⁹ Fang et al. evaluated methanol and ACN buffer modifiers during their HDX-MS study of a complex deuterated *E. coli* lysate.⁵⁰ Separations conducted at subzero temperature have facilitated use of lengthy chromatography gradients of 25–90 min.^{47–50} The 90 min gradient used by Fang et al. yielded ~ 3 -fold more peptide identifications than found for 15 min gradients.

As temperature decreases, practical difficulties with system implementation arise. Chromatography fluids must contain an increasing fraction of buffer modifier, which can introduce complications such as reduced electrospray source ion (ESI) production. Venable et al. reported that sequence coverage of BSA digest peptides declined from 64% to 45% as the volume fraction of EG in the LC solvent reached 40%, corresponding to a -20 °C freezing point. Buffer modifiers can affect system

performance by inducing shorter retention times and diminished resolution,^{47,48} and certain organic buffer modifiers can wash out early eluting peptides.⁵⁰ Increased viscosity of subzero LC fluids at subzero temperature can result in backpressures that exceed the capacity of the LC pump. Phase separations, as occurs in ACN/H₂O mixtures at < -17 °C,⁵¹ may degrade chromatograph performance, although this complication is removed by adding trace EG.⁵²

A distinct challenge to the use of HDX-MS in a QC application is bias from chromatographic carryover, which can adversely affect determinations of $D_{\text{Corrected}}^{\text{Peptide}}(t_{\text{HDX}})$. Chromatographic carryover originates from peptides of prior runs postreleased from the protease, trap, and analytical columns. Because carryover peptides are fully protonated from extended exposure to H₂O, their contributions skew the associated centroid to lower D-content.⁵³ Such contributions can also create false EX1-like kinetics signatures.⁵⁴

Carryover also originates from protein aggregates and agglomerates accumulated at each column entrance. Hamuro and Coales recently reported an HDX-MS valve system that can remove protein particles by backflushing the protease, trap, and analytical columns.⁵⁵ The time devoted to system cleanup of protein residue represents lost productivity, and its duration can exceed that of the HDX-MS measurement.

The HDX-MS interlaboratory comparison for the Fab fragment of NISTmAb found that the $D_{\text{Corrected}}^{\text{Peptide}}(t_{\text{HDX}} > 0)$ in peptides diminished by $\sim 3.5\%$ across measurements of three complete data sets (each set comprised 18 to 24 injections).²¹ Since the larger cohort of laboratories within the HDX-MS study found a reproducibility of $\%E_{\text{Corrected}}^{\text{Peptide}}(t_{\text{HDX}}) = 6.5 \pm 0.6\%$ (all values reported as mean ± 1 standard deviation (SD)), elimination of chromatographic carryover will improve the repeatability, intermediate measurement precision, and reproducibility of HDX-MS.⁵⁶ These precision characteristics are essential attributes of biopharmaceutical QC based on HDX-MS.

This report describes the design of a dual-enzyme, HDX-MS analysis instrument and reports its performance at subzero temperature. The system houses two distinct protease columns that are perpetually cleaned and conditioned while idle. To minimize back-exchange, protein proteolysis is conducted at ≈ 0 °C, and peptides are captured on a trap column and separated on an analytical column at subzero temperature. To minimize noise and chromatographic carryover from peptides trapped on the column and from aggregates and agglomerates, quaternary pumps flush and backflush columns with varied cleaning solutions. For improved data curation, operational temperatures and pressures are recorded and archived with data files. The instrument is integrated into a robotic rail, and the entire system is compatible with the software of the HDX-MS system. The apparatus features stringent temperature regulation, which is little-affected by suboptimal laboratory environments. The instrument is designed to provide uniform results for long-term projects.

■ HDX-MS ANALYSIS APPARATUS DESCRIPTION

System Design. The HDX apparatus comprises a fluidic circuit box conjoined with a commercial robotic rail (Trajan Scientific and Medical, Morrisville, NC) that transports samples and provides automated scheduling for the conduct of HDX experiments. The present dual-enzyme, -30 °C, chromatography instrument is encased in an aerogel insulated steel box of similar dimensions to the original equipment manufacturer

(OEM) box, and it shares the same injection and exit port positions. Consequently, it is a “drop in” replacement for the OEM component. Much of the apparatus was 3D-printed in bronze steel, aluminum, silver, and polylactide (PLA) plastic by in-house and commercial facilities. Mechanical drawings, electrical schematics, parts lists, and STL and EPS file types are available for construction of the dual-enzyme chromatography platform.⁵⁷

The interior of the dual-enzyme, $-30\text{ }^{\circ}\text{C}$, analysis instrument (Figure 1) contains four distinct insulated compartments

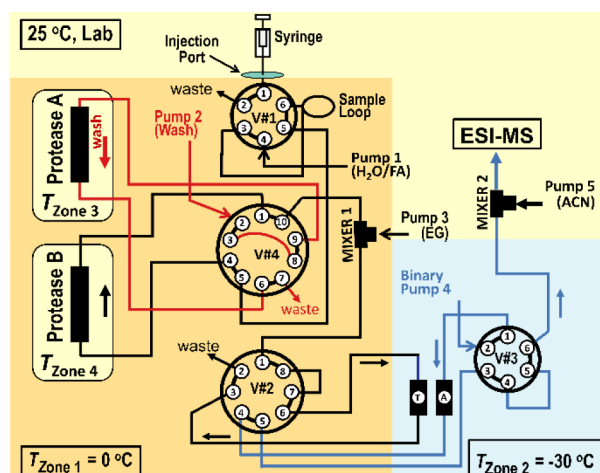


Figure 1. Fluidic circuits of the $-30\text{ }^{\circ}\text{C}$, dual-enzyme HDX-MS instrument.

(referred to as zones), each regulated at a selected temperature. Within each compartment homogeneous temperature is maintained by mounting fluidic and chromatographic components on a 9.6 mm thick aluminum plate. The thermally isolated plates are mounted to a common aluminum frame. The entire system is cooled with a liquid chiller (thermal capacity = 275 W at $-30\text{ }^{\circ}\text{C}$) that circulates solutions containing volume fractions of 30% H_2O /60% EG/10% methanol through 9.53 mm outer diameter (7.75 mm inner diameter) stainless tubing that is clamped and thermally anchored to each aluminum plate. A throttle valve apportions coolant flow between the $0\text{ }^{\circ}\text{C}$ preparation chamber (Zone 1) and subzero analytical chamber (Zone 2). The system cooling capacity is conserved by employing a counter flow heat exchanger in the fluid return circuit of the $0\text{ }^{\circ}\text{C}$ coolant circuit.

Chromatography valves are in thermal contact with their respective aluminum base plates. At solvent entry points and where fluidic circuits pass between Zones 1 and 2, capillaries are clamped to aluminum blocks mounted on a compartment base plate. Capillaries passing from a warm zone to a colder zone have a steady-state temperature profile along their length. Heat is introduced by axial thermal conduction along the capillary and heat advection from liquid flowing through the capillaries. Heat is extracted by forced air convection across unenclosed capillary and conduction through the block. Prior to contacting Valves #1, #3, and #4, thermal modeling estimates that the solvent supply capillaries reach steady state temperature within $0.2\text{ }^{\circ}\text{C}$ of $T_{\text{Zone 1}}$ or $T_{\text{Zone 2}}$. The same model finds that the termini of capillaries passing between Valve #2 and the trap column differ from the local zonal temperature by $<\pm 0.02\text{ }^{\circ}\text{C}$. Interestingly, the forced convection from the compartment fans accounts for a large fraction of total heat transfer.⁵⁸

All other fluidic components (e.g., mixers, analytical columns) are encased in 3D-printed aluminum housings that are mounted to the compartment base plate. Contacts with the thermal mass of a base plate ensure that fluidic components reside at the compartment set point temperature. This isothermal environment suppresses development of a substantial longitudinal temperature increase along columns due to frictional heating between the solvent and column packing.^{59,60}

Two chambers house enzyme columns (Zones 3 and 4). To ensure uniform column temperature, each protease column is mounted into a 3D-printed aluminum or silver collet that fits the enzyme column profile exactly. The collet exterior presents an 8 mm diameter cylinder that is clamped into a holder. Both holders are temperature-regulated independently.

Every 2 s, platinum element resistance temperature detectors (RTDs) and thermistors report to a process controller four compartment temperatures and entrance and exit temperatures of the coolant circulation system. Each coolant circuit has sufficient capacity to chill its aluminum plate below the temperature set point. To maintain each plate at its desired temperature precisely, a proportional–integral–derivative (PID) controller uses a standard negative feedback algorithm to switch DC current to thin-film polyamide encapsulated heaters. In Zones 1 and 2 uniform compartment air temperature is maintained by convective air flows produced by mini-fans.

Compartment temperature profiles recorded during each HDX-MS run are archived with the HDX-MS data. Table 1 lists

Table 1. Typical Temperature Characteristics of the HDX System, Observed during an Operation Period of 0.5 h

zone	T_{avg} $^{\circ}\text{C}$	ΔT_{SD} , ^a $^{\circ}\text{C}$	ΔT_{+} , ^b $^{\circ}\text{C}$	ΔT_{-} , ^b $^{\circ}\text{C}$
1, Preparation	0.000	0.058	0.164	-0.124
2, Analytical	-30.001	0.020	0.054	-0.031
3, Protease A	0.000	0.002	0.004	-0.004
4, Protease B	0.000	0.002	0.004	-0.004

^aUncertainty is 1 standard deviation (SD). ^bDeviation from the average for a minimum duration of 2 s.

typical temperature characteristics of the apparatus during operation. Stringent temperature regulation is demonstrated by small standard deviation, ΔT_{SD} , from T_{Average} in each compartment. Extreme temperature deviations from T_{Average} of at least 2 s duration, ΔT_{+} and ΔT_{-} , are also modest. The same system performance was obtained for laboratory temperatures between 20 and $30\text{ }^{\circ}\text{C}$.

To inhibit water condensation, the box encasing the sample processing apparatus is sealed and purged with dry nitrogen. Two circuits within the six-channel PID controller maintain the heated valve extension shafts above the dew point temperature.

Analysis of a protein sample is initiated by injection of protein solution into a $50\text{ }\mu\text{L}$ sample loop in Zone 1 (Table S1A in the Supporting Information). Actuation of Valve #1 allows Pump 1 ($50\text{ }\mu\text{L}/\text{min}$) to propel the protein sample through protease column A or B, as selected by Valve #4 (Table S1B or S1G). In this valve state peptides pass from the selected protease column (Zone 3 or 4), through Valve #4, and into Mixer 1, where Pump 3 enriches the EG concentration. Peptide solution passes through Valve #2 and into Zone 2, where the peptides are retained on Trap Column T at subzero temperature. Upon subsequent actuations of Valves #2 and #3 (Table S1C), Pump 4 ($50\text{ }\mu\text{L}/\text{min}$) initiates an EG/ H_2O /ACN gradient, which elutes peptides from the trap column and through the analytical

column at subzero temperature. As an option, analytical column effluent passes into Mixer 2, where ACN from Pump 5 ($\sim 50 \mu\text{L}/\text{min}$) increases the total flow to $100 \mu\text{L}/\text{min}$.

The instrument is a flexible platform. The preparation chamber contains a bracket that holds a commercial electrochemical reduction cell.⁶¹ Minor modifications to the fluidic circuits can allow incorporation of an immobilized glycosidase column or immobilized microfluidic enzyme reactor (IMER).^{62–64}

As is required of all chemical kinetic apparatus, system cleanliness is essential for good quality measurements. Accordingly, enzyme columns are stored in place, and a reduced flow of solvent passes through them perpetually. This arrangement also saves start-up time by rendering unnecessary the customary, initial column-conditioning process. During all valve states one or more fluidic components are cleaned (Table S1). Valve #4 selects the enzyme column that is backflushed by Pump 2 (Tables S1B and S1G). While chromatographic gradients are in progress, it is feasible to select either enzyme column for flushing or backflushing (Tables S1C and S1E). Actuations of Valves #2 and #3 allow Pump 4 to backflush the analytical and trap columns (Tables S1D and S1F). Backflushing processes can remove protein particles from column entrances. The use of quaternary pumps allows enzyme column cleaning procedures to include gradients containing chaotropic agents and detergents.

EXPERIMENTAL SECTION

Reagents and Materials. D_2O (99.96 mol % D) was acquired from Cambridge Isotopes (Andover, MA). Sodium phosphate dihydrate, sodium phosphate monohydrate, sodium chloride, and formic acid (FA) were purchased from Sigma-Aldrich (St. Louis, MO). Ethylene glycol ReagentPlus (>99%) was purchased from Alfa Aesar (Ward Hill, MA). The analytical sample used for these experiments was a tryptic digest of fully reduced and iodoacetamide alkylated BSA (Thermo Scientific Pierce BSA Protein Digest Standard, LC–MS grade, catalog no. 88341).

Samples. Undeuterated and fully deuterated peptides were prepared by reconstituting lyophilized BSA peptides in H_2O and D_2O (99.96 mol % D), respectively, with 1% ACN to aid solubility. Peptides with D_2O were kept at 4°C for 1 h to fully exchange. Aliquots of each stock were stored at -80°C . Prior to analysis, samples were diluted in either H_2O or D_2O to $0.05 \text{ pmol}/\text{L}$ and equilibrated at 1°C .

Chromatography. Each LC–MS analysis was initiated by injection of a 2 pmol sample. The peptides were trapped on a C18 column (Phenomenex, Inc.; Torrance, CA; Model Kinetex EVO C18, 100 Å pore, $2.6 \mu\text{m}$ particle size, 20 mm long \times 2.1 mm dia.) and separated on an analytical column (Thermo Fisher Scientific; Waltham, MA; Accucore C18, 80 Å pore, $2.6 \mu\text{m}$ particle size, 30 mm long \times 2.1 mm diameter, catalog no. 17126-032130).

Solvent A comprised mixtures of $\text{H}_2\text{O}/\text{EG}$ and 0.1% FA in volume fractions determined by the working temperature (Table 2). Solvent B comprised volume fractions of 99.9% ACN and 0.1% FA. Solvents A and B combine for a $50 \mu\text{L}/\text{min}$ flow rate. Two LC gradients were used. The short (8 min) gradient was 3–10% B for 0.5 min, 10–50% B for 7.5 min, 50–95% B for 1 min, 95% B for 4 min, 95–3% B for 0.5 min, 3–95% B for 2 min, 95% B for 3 min, and 95–3% B for 0.5 min. The long (40 min) gradient was 3–40% B for 40 min, 40–95% B for 1

Table 2. LC Pump Pressures during Operation of the HDX-MS Analysis System

$T_{\text{Zone } 2}$, $^\circ\text{C}$	solvent A $\text{H}_2\text{O}/\text{EG}$ volume fractions, ^a	$P_{\text{Pump } 1}$, MPa	$P_{\text{Pump } 4}$, MPa
0	100/0	7	24
0	55/45	8	70
–10	74/26	10	40
–20	63/37	20	55
–30	55/45	24	95

^aMixtures contain a volume fraction of 0.1% FA.

min, 95% B for 4 min, 95–15% B for 0.5 min, 15–95% B for 3 min, 95% B for 2 min, and 95–3% B for 1 min.

Mass Spectrometry. Mass spectra were measured by a Thermo Orbitrap Elite (Thermo Fisher Scientific; Waltham, MA). The instrument settings were spray voltage, 3.7 kV; sheath gas flow rate, 25 (arbitrary units); capillary temperature, 275°C . In the Orbitrap stage, MS spectra were acquired with the resolution set at 60000, which has been shown to yield accurate measurements of hydrogen and deuterium composition.⁶⁵ Extracted ion chromatograms (XICs) of undeuterated samples were used for automated peak area calculation in Xcalibur. From mass spectra obtained during HDX-MS experiments, the centroid of each deuterated peptide envelope and the relative deuterium uptake by each peptide was calculated by HDX WorkBench.⁶⁶

Temperature Calibrations. Each RTD and thermistor temperature sensor was calibrated *in situ* against a colocated, K-type thermocouple (Marlin Manufacturing Corp., Cleveland, OH), which had reference junctions immersed in water/ice bath. The vendor calibrated the thermocouples for service between 0 and -40°C per procedures recommend by the National Voluntary Laboratory Accreditation Program (<https://www.nist.gov/nvlap/about-nvlap>).

Estimation of Amide Back-Exchange Rates. Deuterium contents of unstructured peptides in H_2O were estimated by a LabVIEW 7.1 (NI, Austin TX) script. The script reproduced main chain intrinsic hydrogen exchange rates obtained by Excel spreadsheets (<http://hx2.med.upenn.edu/download.html>) containing the 2018 reference parameters.^{7,38,67}

RESULTS AND DISCUSSION

Retained Deuterium in Peptides. The sample in these experiments was perdeuterated tryptic digest of fully reduced and iodoacetamide-treated BSA protein. Except for passage through a protease column, the peptides experienced the solution conditions found in standard bottom-up HDX-MS measurements. This measurement procedure simplifies data interpretation by avoiding possible conflation of chromatographic and proteolytic performance. During these experiments, the apparatus did not use Mixer 2, i.e., the ESI source of the mass spectrometer was directly connected to the analytical column output via Port 6 on Valve #3.

The measurement procedure defined the kinetics model of the analyses. Samples injected into the apparatus sample loop at $t = -3.33 \text{ min}$ resided in Zone 1 (0°C) for 2 min as Pumps 1 and 3 evacuated the sample loop and loaded peptides onto the trap column in Zone 2 ($T_{\text{Zone } 2} = (0, -10, -20, -30)^\circ\text{C}$). Peptides resided on the trap column for 1.33 min during the desalting process. At $t = 0 \text{ min}$, Valves #2 and #3 changed states, enabling Pump 4 to elute peptides from the trap column into the analytical column. An 8 min LC gradient was employed, as it is

Table 3. Percent Deuterium Content in Amide Groups, %D_T^{obs}, of Peptides Chromatographically Separated on the HDX Analysis System for T_{Zone 2} = 0, -10, -20, and -30 °C

volume fraction of EG, % T _{Zone 2} , °C peptide sequence ^a	8 min gradient					40 min gradient	
	0	45	26	37	45	37	45
	0	0	-10	-20	-30	-20	-30
	%D _{0°C} ^{Obs}	%D _{0°C} ^{Obs}	%D _{-10°C} ^{Obs}	%D _{-20°C} ^{Obs}	%D _{-30°C} ^{Obs}	%D _{-20°C} ^{Obs}	%D _{-30°C} ^{Obs}
AEFVEVTK	69.9 ± 0.1	75.9 ± 0.8	79.5 ± 0.3	85.0 ± 0.2	85.1 ± 0.1	83.4 ± 0.1	84.3 ± 0.1
DDSPDLPK	59.8 ± 0.3	67.0 ± 0.2	70.2 ± 0.2	71.0 ± 0.7	69.7 ± 0.6	71.0 ± 0.3	68.2 ± 1.2
DLGEEHFK	42.7 ± 0.2	55.3 ± 0.1	62.8 ± 0.4	70.1 ± 0.2	69.5 ± 0.2	68.0 ± 0.4	67.4 ± 0.4
KQTALVELLK	75.2 ± 0.1	78.1 ± 0.1	82.9 ± 0.1	85.3 ± 0.1	86.0 ± 0.4	83.9 ± 0.2	85.3 ± 0.5
LGEYGFQNALIVR	72.6 ± 1.3	82.9 ± 1.3	84.1 ± 0.9	91.9 ± 0.8	88.6 ± 2.5	87.5 ± 1.2	88.6 ± 1.4
LVNELTEFAK	69.0 ± 0.1	73.2 ± 0.03	80.5 ± 0.1	88.6 ± 0.1	89.4 ± 0.1	84.7 ± 0.2	88.7 ± 0.5
LVVSTQTALA	79.7 ± 0.1	83.9 ± 0.1	88.6 ± 0.2	93.9 ± 0.1	94.8 ± 0.4	92.3 ± 0.1	93.5 ± 0.5
QNC _{CAM} DQFEK	68.0 ± 0.2	81.8 ± 0.3	84.2 ± 0.7	88.6 ± 0.9	84.3 ± 11.1	89.4 ± 0.2	89.7 ± 1.7
QTALVELLK	78.6 ± 0.1	81.4 ± 0.1	84.1 ± 0.1	86.5 ± 0.01	86.7 ± 0.5	85.4 ± 0.2	86.4 ± 0.1
TVMENFVAFVDK	83.0 ± 0.2	85.8 ± 0.6	88.1 ± 0.2	92.7 ± 0.2	90.1 ± 0.4	90.6 ± 0.1	90.5 ± 0.7
YIC _{CAM} DNQDTISSK	69.9 ± 0.2	83.9 ± 0.2	91.2 ± 0.3	101.0 ± 0.2	99.6 ± 0.4	97.9 ± 0.4	97.8 ± 1.3
YLVEIAR	58.5 ± 1.2	64.6 ± 1.1	68.0 ± 0.9	73.9 ± 0.8	69.4 ± 0.9	72.5 ± 0.9	71.3 ± 0.8
(avg) %D _T ^{obs}	68.9 ± 0.5	76.1 ± 0.6	80.3 ± 0.5	85.7 ± 0.5	84.4 ± 3.7	83.9 ± 0.5	84.3 ± 0.9
(avg) %D _T ^{Est}	73.5 ± 0.1	76.8 ± 0.4	83.6 ± 0.3	87.5 ± 0.1	88.8 ± 0.1	86.0 ± 0.1	88.4 ± 0.1
%D _T ^{Obs} Improvement, %D _T ^{Obs} - [%D _{0°C} ^{Obs}] _{8min}		7.2 ± 0.4	11.2 ± 0.3	16.3 ± 0.4	14.9 ± 3.6	14.8 ± 0.4	14.9 ± 1.2
[%D _T ^{Obs}] _{High 3} Improvement,		13.5 ± 0.2	19.2 ± 0.3	26.4 ± 0.4	25.7 ± 0.2	24.9 ± 0.3	24.8 ± 0.4
$\sum_{k=High\ 3} (\%D_{T,k}^{Obs} - [\%D_{0^\circ C,k}^{Obs}]_{8min}) \times \frac{100\%}{3}$							
MAD, %: $\sum_{k=1to12} \frac{ \%D_{T,k}^{Obs} - \%D_{T,k}^{Est} }{\%D_{T,k}^{Est}} \times \frac{100\%}{12}$	11.3 ± 0.6	11.1 ± 0.8	9.3 ± 0.6	9.7 ± 0.5	10.9 ± 2.1	9.5 ± 0.5	11.3 ± 1.2

^aCysteines are carbamidomethylated (CAM).

typical of contemporaneous HDX-MS studies. Experiments conducted with 40 min LC gradients enabled demonstration of the enhanced capabilities offered by operation at subzero temperature.

Chromatographic separations of perdeuterated tryptic digest of BSA were conducted with EG/H₂O mixtures that inhibited freezing in the fluidic circuit. Measurements indicate that charge state distribution did not change with EG concentration; though, the total intensity of the charge state envelope is sensitive to %EG (*vide infra*).

Table 3 lists the percent deuterium content in peptide amide groups, %D_T^{obs}, which were computed using eqs 1 and 2

$$\%D_T^{obs} = \frac{\langle m(t_{HDX}) \rangle^{Peptide} - \Gamma_T^{Peptide}(t_k^{RT})}{(n-1)m_{D^+}} \times 100 \quad (1)$$

$$\Gamma_T^{Peptide}(t_k^{RT}) = \sum_{j=0\ to\ n} a_j R_j^{SC}(T, pH, t_k^{RT})(m_{D^+} - m_{H^+}) \quad (2)$$

where $\langle m(t_{HDX}) \rangle^{Peptide}$ is the centroid mass; t_{HDX} is the immersion time of the sample in D₂O; $\Gamma_T^{Peptide}$ is the estimated deuterium content retained by side chains; t_k^{RT} is the retention time (RT) of the peptide, which are numbered $k = 1, 2, 3...$ in the order of their elution; j is the running index for side chains in the peptide; a_j is the number of identical exchangeable sites within a side chain; R_j^{SC} is the rate expression for deuterium occupancy of the side chain exchangeable site, which is calculated at pH 2.7 and over the temperature history between sample injection into the analysis system ($t = -3.33$ min) and elution, $t_{Peptide}^{RT}$; and m_{D^+} and m_{H^+} are the proton and deuterium masses.

For peptide-containing arginine $\Gamma_T^{SC} \approx 0.96-1.87$ Da, due to deuterium retained at the ϵ -NH ($a_j = 1$) and η -NH₂ ($a_j = 4$) exchangeable sites. Table S2 lists the deuterium mass within the arginine side chains, which were computed with the kinetics model, knowledge of pH, T_{Zone 1}, T_{Zone 2}, peptide retention times (Table S3), and side-chain exchange rate coefficients determined from NMR studies.^{7,68} The known exchange rates of side chains in tryptophan and glutamine predict essentially complete deuterium loss during the proteolysis and desalting processes.⁷ However, because the rate coefficients for acid-catalyzed exchange in some side chains are unreported, %D_T^{obs} should be regarded as the upper limit of deuterium content in peptide amide groups.

The normalizing term, $(n-1)m_{D^+}$, contains n , the number of exchangeable amides, and 1, which represents the N-terminal amide that is exchanged completely. Accordingly, n does not contain contributions from prolines and chemically blocked cysteines.

Table S4 lists estimated percent retained deuterium content in peptide amide groups, %D_T^{Est}, which is computed by the kinetics model with knowledge of pH, T_{Zone 1}, T_{Zone 2}, peptide retention times, amide exchange rates,^{7,38,67} and the $(n-1)m_{D^+}$ normalizing term. We note that %D_T^{Est} does not account for possible deuterium loss in the ion source nor does it contain deuterium mass retained by side chains.^{17,69}

Table 3 lists %D_T^{Obs} and %D_T^{Est}, which are averages of %D_T^{Obs} and %D_T^{Est} across all peptides. These averages show that peptides retain more deuterium as T_{Zone 2} decreases below 0 °C. For T_{Zone 2} < 0 °C, %D_T^{Obs} Improvement ranges between (7.2 ± 0.4) % and (16.3 ± 0.4) %. The reference for this calculation is [%D_{0°C}^{Obs}]_{8min}, which is the %D_T^{Obs} computed for the k peptides

measured during the 8 min gradient at 0 °C. Inspection of $\%D_T^{\text{Obs}}$ for all peptides reveals that improvements of retained deuterium vary as a function of peptide sequence. Thus, Table 3 also reports the $[\%D_T^{\text{Obs}}]_{\text{High3}}$ Improvement measured for the three peptides most affected by chromatographic conditions, which is $(26.4 \pm 0.4) \%$ for an 8 min LC gradient at -20 °C.

Table 3 also reports Relative Mean Absolute Deviation % (MAD), which is the mean of the absolute value differences between $\%D_{T,k}^{\text{Obs}}$ and $\%D_{T,k}^{\text{Est}}$ divided by $\%D_{T,k}^{\text{Est}}$ across all peptides. The ratios reveal that $\%D_{T,k}^{\text{Obs}}$ and $\%D_{T,k}^{\text{Est}}$ differ by $(9.3 \pm 0.6) \%$ to $(11.3 \pm 1.2) \%$ across all temperatures, which is within the expected accuracy of the calculations.

$\%D_T^{\text{Est}}$ overestimates $\%D_T^{\text{Obs}}$ for 57% of peptides. Greater discord was expected. Previously, Woodward et al. reported that addition of EG to water decreased exchange rates in folded proteins at 20 °C.⁷⁰ No model for effects of EG on exchange rates, validated against data, was developed; however, it was proposed that exchange rates in EG/H₂O mixtures at a given pH and temperature are affected by the volume fraction of water, the water equilibrium constant (k_w), and the dielectric constant. Since these effects may be offsetting, this ostensive small bias in $\%D_T^{\text{Est}}$ may be fortuitous.

This study found essentially the same $\%D_T^{\text{Obs}}$ and $\%D_T^{\text{Est}}$ for BSA peptides observed during chromatography at -20 and -30 °C for 8 min (EW ≈ 3.5 min) and 45 min gradients (EW ≈ 22 min), where EW is the elution window defined by the time interval between elution of the first (t_1^{RT}) and last (t_{12}^{RT}) LC peaks. Simulations predict that separations conducted using longer gradients will show greater differences. Table S5 lists $\%D_T^{\text{Est}}$ estimated for the same BSA peptides separated at -20 °C and -30 °C with 90 and 120 min gradients. For these estimates the BSA peptide retention times t_k^{RT} are stretched to fill the gradient duration in proportion to retention times listed in Table S3 for 40 min gradients at -20 °C and -30 °C, i.e., $t_1^{\text{RT,new}} = t_1^{\text{RT,40 min}}$ and $t_{12}^{\text{RT,new}} = t_{12}^{\text{RT,40 min}} + \text{EW}$. For lengthy gradients, the improvement for conducting the separation at -30 °C vs -20 °C is $\approx 5.5\%$ for a 90 min gradient and $\approx 7\%$ for a 120 min gradient.

Solution %EG and Temperature Affect Chromatographic Performance. Adding EG to solvent A of analytical Pump 4 resulted in earlier elution of peptides (Figure 2). For example, when conducting 8 min gradients at $T_{\text{Zone } 2} = 0$ °C, solutions containing volume fractions of 45% EG eluted peptides approximately 1–3 min earlier than observed with 0% EG (Table S3).

Contrariwise, a decrease in temperature is known to increase retention time for most analytes. Such retention time shifts were observed as $T_{\text{Zone } 2}$ was sequentially decreased from 0 to -30 °C (Table S3). In a volume fraction of 45% EG solution peptide elution times shift by ~ -0.2 min to $\sim +2.2$ min as $T_{\text{Zone } 2}$ decreases from 0 to -30 °C.

While retention times shifted with respect to volume fraction of EG and temperature, peptide separation was not negatively impacted. Under all conditions evaluated, chromatographic peak shapes during 8 min gradients exhibited minimal change (Figure 2). Figure 2A shows representative peaks observed for YLYEIAR²⁺ during separation in volume fractions of 45% EG and 0% EG at $T_{\text{Zone } 2} = 0$ °C. The LC peak eluted with 45% EG had similar width and greater peak area than the LC peak eluted with 0% EG. At $T_{\text{Zone } 2} = -30$ °C, the full-width half-maximum

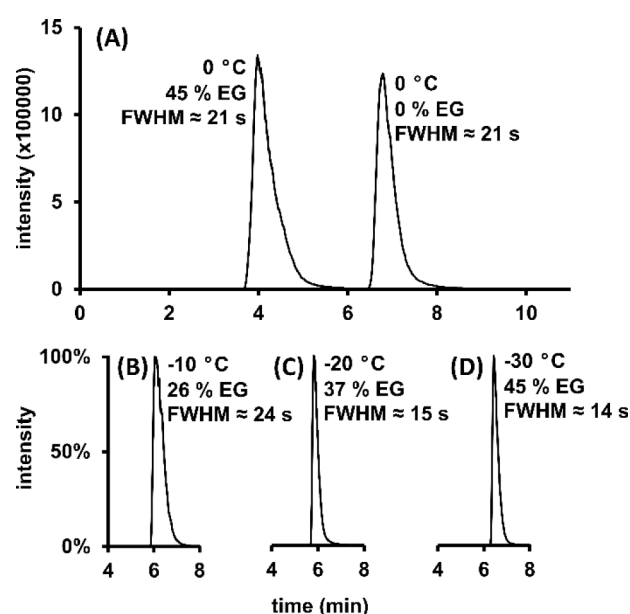


Figure 2. Chromatographic peaks of peptide YLYEIAR²⁺ recorded during 8 min gradients: (A) 0 °C, 45% EG and 0% EG, (B) -10 °C, 26% EG, (C) -20 °C, 37% EG, and (D) -30 °C, 45% EG.

(fwhm) peak width was (14 ± 2) s and retention time was comparable to 0% EG at $T_{\text{Zone } 2} = 0$ °C (Figure 2D).

A factor affecting LC peak widths is temperature inhomogeneity within the analytical column.^{59,71–74} Installation of columns in high conductivity metal cases in contact with the $T_{\text{Zone } 2}$ thermal reservoir establishes nearly isothermal longitudinal temperature profiles. However, heat produced by friction between the solvent and the porous column medium produces a radially symmetric temperature profile with its maximum on the column axis, $T_{\text{Axis}} > T_{\text{Zone } 2}$, and its minimum at the wall boundary, $T_{\text{Wall}} = T_{\text{Zone } 2}$. The radial temperature profile gives rise to inhomogeneous transport and release kinetics between the analyte and column packing. This amount of inhomogeneity appears to have little effect, as the YLYEIAR²⁺ peptide peak width is rangebound between 14 and 24 s. The estimated radial temperature difference is $(T_{\text{Axis}} - T_{\text{Wall}}) \leq 0.1$ °C, assuming incompressible solvents.⁶⁰

As $T_{\text{Zone } 2}$ decreases to -30 °C, the viscosity of EG/ACN/H₂O mixtures increases and pressures at the trap and analytical columns increase proportionately (Table 2). Consequently, the pressure capacity of Pump 4 largely governs choice of analytical column dimensions and particle size. During this study, the maximum pressure at Pump 4 was 95 MPa, which is within the pressure capacity of some commercial LC pumps. Pump 4 can drive 151.8 MPa; however, for chromatography this pressure must be derated slightly to accommodate pressure surges from valve switching. This pump has successfully driven LC gradients at -30 °C with a 5 μm particle size, 4 mm \times 2.1 mm diameter trap column and a 1.9 μm particle size, 50 mm long \times 1 mm diameter analytical column. However, the present configuration appeared to provide the best combination of resolution and sensitivity.

Effects of EG and Added ACN on MS. EG is significantly more viscous than water and not a common solvent for MS. To evaluate the effect of EG on ion intensity during ESI-MS analyses, the integrated area of the extracted ion chromatogram (XIC) for each peptide separated on the analytical column at $T_{\text{Zone } 4} = 0$ °C was tabulated (Table S6). Triplicate measure-

ments were conducted. $A_{0\%EG}$ is the peak area of a peptide eluted using solvent A that contains volume fractions of 99.9% $H_2O/0.1\%FA$, which is a mixture used for conventional LC–MS. $A_{45\%EG}$ is the peak area of a peptide eluted using solvent A that contains volume fractions of 45% EG/54.99% $H_2O/0.1\%FA$. The ratio of peak areas for each peptide eluted under the two solvent A conditions is

$$R_3 = \frac{A_{45\%EG}}{A_{0\%EG}} \times 100 \quad (3)$$

Unshaded bars in Figure 3 plot the R_3 ratios determined from the XIC data. Ratios greater than 100% indicate greater detected

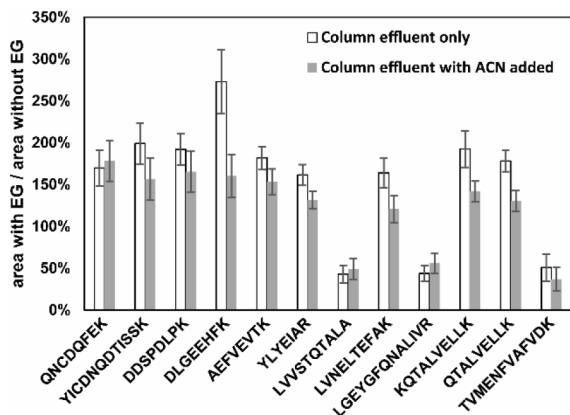


Figure 3. Peak areas of 12 peptides observed from an electrospray ion source that is sampling analytical column effluent ($50 \mu\text{L}/\text{min}$) comprising $H_2O/EG/ACN$ (unshaded bars) and analytical column effluent that is supplemented with $50 \mu\text{L}/\text{min}$ ACN for a combined flow of $100 \mu\text{L}/\text{min}$ (shaded bars). Peak areas for both conditions are normalized to the peak areas of the conventional condition without EG. Peptides are listed left to right in the order of retention time. Error bars indicate SD of triplicate measurements.

ion intensity for peptides eluted in solvent A solutions containing volume fractions of 45% EG. For the 12 selected peptides, nine peptides showed improved performance and three peptides showed reduced performance with EG.

Since ESI is often improved for solutions containing large fractions of ACN and ACN reduces viscosity of H_2O/EG mixtures, Mixer 2 was added to the fluidic circuit, and the effect of supplemental ACN on ESI yield was measured. At Mixer 2, the $50 \mu\text{L}/\text{min}$ analytical column effluent flow was combined with the $50 \mu\text{L}/\text{min}$ flow from Pump 5, which comprised volume fractions of 99.9% ACN and 0.1% FA. The resulting $100 \mu\text{L}/\text{min}$

flow entered the ESI source. The resulting XIC yields $A_{45\%EG+ACN}$, which is normalized by $A_{0\%EG}$:

$$R_4 = \frac{A_{45\%EG+ACN}}{A_{0\%EG}} \times 100 \quad (4)$$

In Figure 3, shaded bars labeled “Column effluent with ACN added” present the R_4 ratios. Since most ratios are $<100\%$, we conclude that supplementing $50 \mu\text{L}/\text{min}$ column flow with $50 \mu\text{L}/\text{min}$ ACN provides no net increase of signal intensity. This minimal impact may be due to the relatively low flow rate of $50 \mu\text{L}/\text{min}$, which suitably desolvated ions during ESI even with EG (Table S6).

Many HDX-MS users operate with flow rates around $200 \mu\text{L}/\text{min}$, which may benefit from an addition of ACN. A common approach to improve ESI efficiency is to use a heated probe at higher flow rates. This is not advisable for HDX-MS, as the excess heat applied can increase back-exchange.^{17,69} Addition of ACN prior to ESI may serve as an alternative strategy for probes at ambient temperature and for MS instrumentation with different source configurations.

Previously, Venable et al. reported that ion intensity declined as the EG concentration in the ESI solution increased to 45%.⁴⁷ In contrast, the present data indicate that BSA peptide ion intensities mainly remain stable or increase as the EG concentration is increased. The discord between the present and prior reports does not reside in differences of chromatography apparatus, as the present peptide ion intensity trends are also observed for BSA peptides in EG/ H_2O/FA solutions infused directly by a syringe pump. We speculate that the generational differences between the older and present ESI source configurations account for the stable performance reported in this work.

Subzero $T_{\text{Zone } 2}$ Expands the LC Elution Window. Performance parameters of HDX-MS apparatus include $\%D_T^{\text{Est}}(0)$, the estimated average deuterium content in peptides at the onset of the LC gradient; *LC Peak Width*, the temporal width of eluting LC peaks (fwhm); LC retention time of a peptide (defined above); $\%D_T^{\text{Est}}(t_1^{\text{Obs}})$, the estimated average deuterium content in all peptides at the start of the elution window; *EW*, the elution window; and $\Delta\%D_T^{\text{Est}}(EW)$, the estimated average deuterium content change of the peptide set during the elution window, which is, effectively, the bias across the set of $D_{\text{Uncorrected}}^{\text{Peptide}}(t_k^{\text{RT}})$. Table 4 lists these properties for the reported solution conditions.

Table 4. HDX-MS Characteristics at $T_{\text{Zone } 2} \leq 0^\circ\text{C}$

$T_{\text{Zone } 2}$ ($^\circ\text{C}$)	volume fraction of EG (%)	LC Grad (min)	$\overline{\%D_T^{\text{Est}}(0)}^a$ (%)	LC Peak Width (fwhm) (s)	t_1^{RT} (min)	$\overline{\%D_T^{\text{Est}}(t_1^{\text{RT}})}^b$ (%)	EW (min)	$\Delta\%D_T^{\text{Est}}(EW)$ (%) ^c
0	0	8	85.6	21 ± 2	5.52 ± 0.03	75.2 ± 0.1	3.30 ± 0.02	-4.6 ± 0.2
0	45	8	85.6	21 ± 2	2.54 ± 0.06	80.3 ± 0.2	4.80 ± 0.04	-7.7 ± 0.4
-10	26	8	88.1	24 ± 2	4.42 ± 0.14	84.7 ± 0.1	3.50 ± 0.10	-2.3 ± 0.1
-20	37	8	89.0	15 ± 2	3.48 ± 0.02	88.1 ± 0.1	4.40 ± 0.02	-1.0 ± 0.1
-30	45	8	89.2	14 ± 2	3.30 ± 0.11	89.0 ± 0.1	5.30 ± 0.07	-0.3 ± 0.1
-20	37	40	89.0	17 ± 2	3.60 ± 0.25	88.1 ± 0.1	22.2 ± 0.18	-5.7 ± 0.2
-30	45	40	89.2	22 ± 2	3.27 ± 0.32	89.0 ± 0.1	20.4 ± 0.23	-1.3 ± 0.2

^aEstimate assumes no temporal dispersion prior to LC chromatography ($t < 0$ min). ^bUncertainty includes contributions from uncertainty of t_1^{EW} .

^cUncertainty includes contributions from the sum of *EW* uncertainty and one *LC Peak Width*.

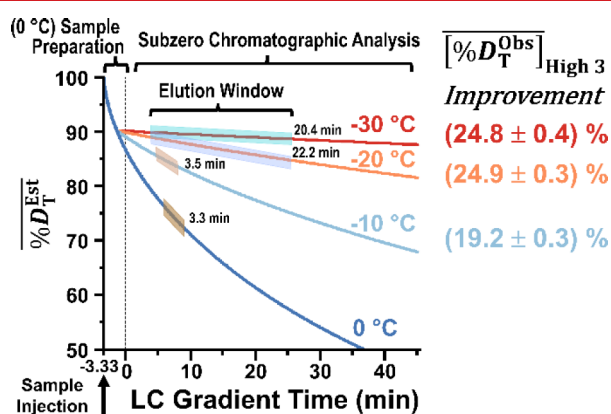


Figure 4. $\overline{\%D_T^{\text{Est}}}$ vs LC Gradient Time (min) computed for the 12-peptide set separated by liquid chromatography at 0, -10, -20, and -30 °C, at pH 2.7, and conditions listed in Table 3. The shaded area along each plot of $\overline{\%D_T^{\text{Est}}}$ marks the observed elution window for all peptides. The right column lists the average $[\%D_T^{\text{Obs}}]_{\text{High3}}$ Improvement, referenced to 8 min gradient data observed at 0 °C, for $T_{\text{Zone } 2}$ (LC gradient duration): -10 °C (8 min), -20 °C (40 min), and -30 °C (40 min).

Figure 4 plots $\overline{\%D_T^{\text{Est}}}$ vs LC Gradient Time for 12 peptides at $T_{\text{Zone } 2} = (0, -10, -20, -30)$ °C. Plots of $\overline{\%D_T^{\text{Est}}}$ during negative time estimates the average deuterium content as perdeuterated protein undergoes proteolysis and desalting. After protein proteolysis for 2 min at 0 °C, the kinetics model estimates $\overline{\%D_T^{\text{Est}}}$ (-1.33 min) = 89.3%. When operating at $T_{\text{Zone } 2} = -30$ °C, peptides enter the analytical column containing $\overline{\%D_T^{\text{Est}}}(0) = 89.2\%$ of the initial deuterium content, which is 3.6% more deuterium than retained by peptides desalted at 0 °C (Table 4).

Additional deuterium content is lost before elution of the first LC peak. The estimated loss is $\overline{\%D_T^{\text{Est}}}(t_1^{\text{RT}}) \approx 10.4\%$ when $T_{\text{Zone } 2} = 0$ °C and $\overline{\%D_T^{\text{Est}}}(t_1^{\text{RT}}) \approx 0.2\%$ for $T_{\text{Zone } 2} = -30$ °C. Consequently, HDX-MS instruments operating at subzero temperatures feature greater dynamic range for determination of $\overline{\%D_T^{\text{Obs}}}$ than conventional instruments operating at 0 °C.

HDX-MS experiments have used short LC gradients to limit losses of deuterium due to back-exchange. For example, the 15 laboratories that contributed data to the NIST HDX-MS interlaboratory study employed LC gradients of (6.5 to 9.5) min.²¹ The present 8 min gradient used to separate perdeuterated BSA digest peptides exhibited an elution window of 3.3 min at 0 °C (Figure 4, Table 4). Short LC elution windows are often congested with overlapping peaks. This congestion can hinder peptide identifications. Temporally coincident LC peaks with overlapping isotopic envelopes can corrupt determination of centroid masses and sequences. Overlapping peaks can suffer from ion suppression of eluents. These issues can limit the mass of proteins accessible to HDX-MS experiments.¹⁹

Operation of a chromatograph at subzero temperature allows the operator to expand LC elution windows with no back-exchange penalty (Table 4). As shown in Figure 4, analyses of BSA tryptic digest with 40 min gradients at $T_{\text{Zone } 2} = -20$ and -30 °C have LC elution windows of 20.4 and 22.2 min,

respectively. For $T_{\text{Zone } 2} = -30$ °C the change in average deuterium content of the peptide set is $\Delta\overline{\%D_T^{\text{Est}}}(EW) = (-1.3 \pm 0.2)\%$ during a 40 min gradient, which is $\sim 28\%$ of deuterium loss suffered by the peptide set during an 8 min gradient at $T_{\text{Zone } 2} = 0$ °C (Table 4). Thus, when separated at -30 °C in 45% EG using a 40 min chromatographic gradient, peptides exhibiting rapid back-exchange can exhibit $\approx 25\%$ greater deuterium content than the same peptides separated at 0 °C, 0% EG using an 8 min gradient (Table 3).

CONCLUSION

The present report describes the design of a dual-enzyme HDX-MS analysis instrument and exploration its performance at subzero temperature. This instrument offers greater dynamic range for determinations of $\overline{\%D_T^{\text{Obs}}}$ with reduced back-exchange. The system is a versatile metrology platform for HDX-MS of proteins. Dual enzyme columns can support investigations requiring multiple proteases that produce overlapping peptide sequences^{75–77} and the study of glycoproteins requiring protease and glycosidase columns. Plans for this instrument and its electronics are archived in a public repository.⁵⁷

The design and operational capabilities minimize effects of bias, variance, and drift during determination of each $D_{\text{corrected}}^{\text{peptide}}(t_{\text{HDX}})$. The fluidic architecture supports system cleanliness by flushing and backflushing columns and by cleaning cycles with quaternary pumps. The ability to conduct cleaning cycles during analytical chromatography gradients will shorten the duration of measurement campaigns, optimizing valuable instrument use. Rigorous temperature control will enable an HDX-MS analysis system to provide the same fluidic environment for extended timeframes, enhancing repeatability and intermediate measurement precision.⁵⁶ Temperature logging with each HDX-MS measurement provides a record that will support computational modeling of measurements. These features will enable the dual-enzyme, subzero, HDX-MS instrument to become a reliable platform for future biopharmaceutical QC programs and protein similarity studies based on HDX-MS.

ASSOCIATED CONTENT

Supporting Information

The Supporting Information is available free of charge at <https://pubs.acs.org/doi/10.1021/jasms.2c00096>.

Table of fluidic circuits and operational valve states of the dual-enzyme HDX-MS instrument; table of calculated side-chain deuterium content in arginine for $T \leq 0$ °C LC conditions; table of retention times observed for selected BSA peptides at $T \leq 0$ °C LC conditions; table of $\overline{\%D_T^{\text{Est}}}$ for selected BSA peptides for $T \leq 0$ °C LC conditions; table comparing LC-MS signal intensities of selected BSA peptides that were eluted in solutions containing 0% EG and 45% EG and for ESI mixtures prepared by mixing ACN with column effluent containing 45% EG (PDF)

AUTHOR INFORMATION

Corresponding Author

Jeffrey W. Hudgens – National Institute of Standards and Technology, Bioprocess Measurement Group, Biomolecular Measurements Division, Rockville, Maryland 20850, United States; Institute for Bioscience and Biotechnology Research, Rockville, Maryland 20850, United States; orcid.org/0000-0003-2805-1048; Email: jeffrey.hudgens@nist.gov

Author

Kyle W. Anderson – National Institute of Standards and Technology, Bioprocess Measurement Group, Biomolecular Measurements Division, Rockville, Maryland 20850, United States; Institute for Bioscience and Biotechnology Research, Rockville, Maryland 20850, United States; orcid.org/0000-0002-2808-3026

Complete contact information is available at:
<https://pubs.acs.org/10.1021/jasms.2c00096>

Author Contributions

The manuscript was written by the coauthors. Both authors have approved the final version of the manuscript.

Notes

Certain commercial materials and equipment are identified to adequately specify experimental procedures. Such identifications neither imply recommendation or endorsement by the National Institute of Standards and Technology nor does it imply that the material or equipment identified is the best available for the purpose.

The authors declare no competing financial interest.

ACKNOWLEDGMENTS

J.W.H. acknowledges Dr. Dean Ripple for his technical advice on temperature control strategies, Jawad Pashmi (Thermo Fisher Scientific; Waltham, MA) for technical assistance with the LC apparatus, and Stephen Coales (Trajan Scientific and Medical, Morrisville, NC) for technical advice and discussions during this work.

REFERENCES

- (1) Weis, D. D.: *Hydrogen Exchange Mass Spectrometry of Proteins: Fundamentals, Methods, and Applications*, 1st ed.; Weis, D. D., Ed.; John Wiley & Sons, Ltd.: Chichester, 2016.
- (2) Pirrone, G. F.; Iacob, R. E.; Engen, J. R. Applications of Hydrogen/Deuterium Exchange MS from 2012 to 2014. *Anal. Chem.* **2015**, *87* (1), 99–118.
- (3) Engen, J. R.; Botzanowski, T.; Peterle, D.; Georgescauld, F.; Wales, T. E. Developments in Hydrogen/Deuterium Exchange Mass Spectrometry. *Anal. Chem.* **2021**, *93* (1), 567–582.
- (4) Visser, J.; Feuerstein, I.; Stangler, T.; Schmiederer, T.; Fritsch, C.; Schiestl, M. Physicochemical and Functional Comparability Between the Proposed Biosimilar Rituximab GP2013 and Originator Rituximab. *BioDrugs* **2013**, *27* (5), 495–507.
- (5) Wei, H.; Mo, J.; Tao, L.; Russell, R. J.; Tymiak, A. A.; Chen, G.; Iacob, R. E.; Engen, J. R. Hydrogen/deuterium exchange mass spectrometry for probing higher order structure of protein therapeutics: methodology and applications. *Drug Discovery Today* **2014**, *19* (1), 95–102.
- (6) Rogstad, S.; Faustino, A.; Ruth, A.; Keire, D.; Boyne, M.; Park, J. A Retrospective Evaluation of the Use of Mass Spectrometry in FDA Biologics License Applications. *J. Am. Soc. Mass Spectrom.* **2017**, *28* (5), 786–794.
- (7) Bai, Y. W.; Milne, J. S.; Mayne, L.; Englander, S. W. Primary Structure Effects on Peptide Group Hydrogen-Exchange. *Proteins: Struct. Funct. Genet.* **1993**, *17* (1), 75–86.
- (8) Ehring, H. Hydrogen exchange electrospray ionization mass spectrometry studies of structural features of proteins and protein/protein interactions. *Anal. Biochem.* **1999**, *267* (2), 252–259.
- (9) Lam, T. T.; Lanman, J. K.; Emmett, M. R.; Hendrickson, C. L.; Marshall, A. G.; Prevelige, P. E. Mapping of protein:protein contact surfaces by hydrogen/deuterium exchange, followed by on-line high-performance liquid chromatography-electrospray ionization Fourier-transform ion-cyclotron-resonance mass analysis. *J. Chromatogr. A* **2002**, *982* (1), 85–95.
- (10) Emmett, M. R.; Kazacic, S.; Marshall, A. G.; Chen, W.; Shi, S. D. H.; Bolaños, B.; Greig, M. J. Supercritical Fluid Chromatography Reduction of Hydrogen/Deuterium Back Exchange in Solution-Phase Hydrogen/Deuterium Exchange with Mass Spectrometric Analysis. *Anal. Chem.* **2006**, *78* (19), 7058–7060.
- (11) Kaltashov, I. A.; Bobst, C. E.; Abzalimov, R. R. H/D exchange and mass spectrometry in the studies of protein conformation and dynamics: is there a need for a top-down approach? *Anal. Chem.* **2009**, *81* (19), 7892–7899.
- (12) Zhang, H. M.; Bou-Assaf, G. M.; Emmett, M. R.; Marshall, A. G. Fast Reversed-Phase Liquid Chromatography to Reduce Back Exchange and Increase Throughput in H/D Exchange Monitored by FT-ICR Mass Spectrometry. *J. Am. Soc. Mass Spectrom.* **2009**, *20* (3), 520–524.
- (13) Zhang, Z. Q.; Zhang, A.; Xiao, G. Improved Protein Hydrogen/Deuterium Exchange Mass Spectrometry Platform with Fully Automated Data Processing. *Anal. Chem.* **2012**, *84* (11), 4942–4949.
- (14) Bobst, C. E.; Kaltashov, I. A. Enhancing the Quality of H/D Exchange Measurements with Mass Spectrometry Detection in Disulfide-Rich Proteins Using Electron Capture Dissociation. *Anal. Chem.* **2014**, *86* (11), 5225–5231.
- (15) Valeja, S. G.; Emmett, M. R.; Marshall, A. G. Polar Aprotic Modifiers for Chromatographic Separation and Back-Exchange Reduction for Protein Hydrogen/Deuterium Exchange Monitored by Fourier Transform Ion Cyclotron Resonance Mass Spectrometry. *J. Am. Soc. Mass Spectrom.* **2012**, *23* (4), 699–707.
- (16) Ahn, J.; Jung, M. C.; Wyndham, K.; Yu, Y. Q.; Engen, J. R. Pepsin Immobilized on High-Strength Hybrid Particles for Continuous-Flow Online Digestion at 10 000 psi. *Anal. Chem.* **2012**, *84* (16), 7256–7262.
- (17) Walters, B. T.; Ricciuti, A.; Mayne, L.; Englander, S. W. Minimizing Back Exchange in the Hydrogen Exchange-Mass Spectrometry Experiment. *J. Am. Soc. Mass Spectrom.* **2012**, *23* (12), 2132–2139.
- (18) Nazari, Z. E.; van de Weert, M.; Bou-Assaf, G.; Houde, D.; Weiskopf, A.; Rand, K. D. Rapid Conformational Analysis of Protein Drugs in Formulation by Hydrogen/Deuterium Exchange Mass Spectrometry. *J. Pharm. Sci.* **2016**, *105* (11), 3269–3277.
- (19) Engen, J. R.; Wales, T. E. Analytical Aspects of Hydrogen Exchange Mass Spectrometry. In *Annual Review of Analytical Chemistry*; Cooks, R. G., Pemberton, J. E. Eds.; Annual Reviews; 2015; Vol. 8, pp 127–148.
- (20) Gallagher, E. S.; Hudgens, J. W. Mapping Protein–Ligand Interactions with Proteolytic Fragmentation, Hydrogen/Deuterium Exchange-Mass Spectrometry. In *Methods in Enzymology*; Kelman, Z., Ed.; Academic Press, 2016; Vol. 566, Chapter 14, pp 357–404.
- (21) Hudgens, J. W.; Gallagher, E. S.; Karageorgos, I.; Anderson, K. W.; Filliben, J. J.; Huang, R. Y. C.; Chen, G.; Bou-Assaf, G. M.; Espada, A.; Chalmers, M. J.; et al. Interlaboratory Comparison of Hydrogen–Deuterium Exchange Mass Spectrometry Measurements of the Fab Fragment of NISTmAb. *Anal. Chem.* **2019**, *91* (11), 7336–7345.
- (22) Bobst, C. E.; Abzalimov, R. R.; Houde, D.; Kloczewiak, M.; Mhatre, R.; Berkowitz, S. A.; Kaltashov, I. A. Detection and characterization of altered conformations of protein pharmaceuticals using complementary mass spectrometry-based approaches. *Anal. Chem.* **2008**, *80* (19), 7473–7481.
- (23) Houde, D.; Arndt, J.; Domeier, W.; Berkowitz, S.; Engen, J. R. Characterization of IgG1 Conformation and Conformational Dynamics by Hydrogen/Deuterium Exchange Mass Spectrometry. *Anal. Chem.* **2009**, *81* (14), 5966–5966.
- (24) Rey, M.; Mrazek, H.; Pompach, P.; Novak, P.; Pelosi, L.; Brandolin, G.; Forest, E.; Havlicek, V.; Man, P. Effective Removal of Nonionic Detergents in Protein Mass Spectrometry, Hydrogen/Deuterium Exchange, and Proteomics. *Anal. Chem.* **2010**, *82* (12), 5107–5116.
- (25) Houde, D.; Berkowitz, S. A.; Engen, J. R. The Utility of Hydrogen/Deuterium Exchange Mass Spectrometry in Biopharmaceutical Comparability Studies. *J. Pharm. Sci.* **2011**, *100* (6), 2071–2086.

- (26) Marciano, D. P.; Dharmarajan, V.; Griffin, P. R. HDX-MS guided drug discovery: small molecules and biopharmaceuticals. *Curr. Opin. Struct. Biol.* **2014**, *28*, 105–111.
- (27) Majumdar, R.; Middaugh, C. R.; Weis, D. D.; Volkin, D. B. Hydrogen-Deuterium Exchange Mass Spectrometry as an Emerging Analytical Tool for Stabilization and Formulation Development of Therapeutic Monoclonal Antibodies. *J. Pharm. Sci.* **2015**, *104* (2), 327–345.
- (28) Leurs, U.; Mistarz, U. H.; Rand, K. D. Getting to the core of protein pharmaceuticals - Comprehensive structure analysis by mass spectrometry. *Eur. J. Pharm. Biopharm.* **2015**, *93*, 95–109.
- (29) Deng, B.; Lento, C.; Wilson, D. J. Hydrogen deuterium exchange mass spectrometry in biopharmaceutical discovery and development - A review. *Anal. Chim. Acta* **2016**, *940*, 8–20.
- (30) Trabjerg, E.; Nazari, Z. E.; Rand, K. D. Conformational analysis of complex protein states by hydrogen/deuterium exchange mass spectrometry (HDX-MS): Challenges and emerging solutions. *TrAC, Trends Anal. Chem.* **2018**, *106*, 125–138.
- (31) Hamuro, Y. Quantitative Hydrogen/Deuterium Exchange Mass Spectrometry. *J. Am. Soc. Mass Spectrom.* **2021**, *32* (12), 2711–2727.
- (32) Zhang, Z.; Smith, D. L. Determination of amide hydrogen exchange by mass spectrometry: A new tool for protein structure elucidation. *Protein Sci.* **1993**, *2*, 522–531.
- (33) Mayne, L. Hydrogen Exchange Mass Spectrometry. In *Methods in Enzymology*; Kelman, Z., Ed.; Vol. 566; Academic Press, 2016; Chapter 13, pp 335–356.
- (34) Sheff, J. G.; Rey, M.; Schriemer, D. C. Peptide–Column Interactions and Their Influence on Back Exchange Rates in Hydrogen/Deuterium Exchange-MS. *J. Am. Soc. Mass Spectrom.* **2013**, *24* (7), 1006–1015.
- (35) Burkitt, W.; O'Connor, G. Assessment of the repeatability and reproducibility of hydrogen/deuterium exchange mass spectrometry measurements. *Rapid Commun. Mass Spectrom.* **2008**, *22* (23), 3893–3901.
- (36) Rand, K. D.; Lund, F. W.; Amon, S.; Jørgensen, T. J. D. Investigation of amide hydrogen back-exchange in Asp and His repeats measured by hydrogen ($^1\text{H}/^2\text{H}$) exchange mass spectrometry. *Int. J. Mass Spectrom.* **2011**, *302* (1), 110–115.
- (37) Molday, R. S.; Englander, S. W.; Kallen, R. G. Primary structure effects on peptide group hydrogen exchange. *Biochem.* **1972**, *11* (2), 150–158.
- (38) Nguyen, D.; Mayne, L.; Phillips, M. C.; Walter Englander, S. Reference Parameters for Protein Hydrogen Exchange Rates. *J. Am. Soc. Mass Spectrom.* **2018**, *29* (9), 1936–1939.
- (39) Wales, T. E.; Eggertson, M. J.; Engen, J. R. Considerations in the Analysis of Hydrogen Exchange Mass Spectrometry Data. In *Mass Spectrometry Data Analysis in Proteomics. Methods in Molecular Biology (Methods and Protocols)*, Matthiesen, R., Ed.; Humana Press, 2013; Vol. 1007, pp 263–288.
- (40) Kan, Z. Y.; Mayne, L.; Chetty, P. S.; Englander, S. W. ExMS: Data Analysis for HX-MS Experiments. *J. Am. Soc. Mass Spectrom.* **2011**, *22* (11), 1906–1915.
- (41) Kan, Z. Y.; Walters, B. T.; Mayne, L.; Englander, S. W. Protein hydrogen exchange at residue resolution by proteolytic fragmentation mass spectrometry analysis. *Proc. Natl. Acad. Sci. U. S. A.* **2013**, *110* (41), 16438–16443.
- (42) Gessner, C.; Steinchen, W.; Bédard, S.; J. Skinner, J.; Woods, V. L.; Walsh, T. J.; Bange, G.; Pantazatos, D. P. Computational method allowing Hydrogen-Deuterium Exchange Mass Spectrometry at single amide Resolution. *Sci. Rep.* **2017**, *7* (1), 3789.
- (43) Kan, Z. Y.; Ye, X.; Skinner, J. J.; Mayne, L.; Englander, S. W. ExMS2: An Integrated Solution for Hydrogen-Deuterium Exchange Mass Spectrometry Data Analysis. *Anal. Chem.* **2019**, *91* (11), 7474–7481.
- (44) Amon, S.; Trelle, M. B.; Jensen, O. N.; Jørgensen, T. J. D. Spatially Resolved Protein Hydrogen Exchange Measured by Subzero-Cooled Chip-Based Nano-electrospray Ionization Tandem Mass Spectrometry. *Anal. Chem.* **2012**, *84* (10), 4467–4473.
- (45) Pan, J. X.; Zhang, S. P.; Parker, C. E.; Borchers, C. H. Subzero Temperature Chromatography and Top-Down Mass Spectrometry for Protein Higher-Order Structure Characterization: Method Validation and Application to Therapeutic Antibodies. *J. Am. Chem. Soc.* **2014**, *136* (37), 13065–13071.
- (46) Pan, J. X.; Zhang, S. P.; Borchers, C. H. Comparative higher-order structure analysis of antibody biosimilars using combined bottom-up and top-down hydrogen-deuterium exchange mass spectrometry. *Biochim. Biophys. Acta, Proteins Proteomics* **2016**, *1864* (12), 1801–1808.
- (47) Venable, J. D.; Okach, L.; Agarwalla, S.; Brock, A. Subzero Temperature Chromatography for Reduced Back-Exchange and Improved Dynamic Range in Amide Hydrogen/Deuterium Exchange Mass Spectrometry. *Anal. Chem.* **2012**, *84* (21), 9601–9608.
- (48) Wales, T. E.; Fadgen, K. E.; Eggertson, M. J.; Engen, J. R. Subzero Celsius separations in three-zone temperature controlled hydrogen deuterium exchange mass spectrometry. *J. Chromatogr. A* **2017**, *1523*, 275–282.
- (49) Zhang, Q.; Yang, J.; Bautista, J.; Badithe, A.; Olson, W.; Liu, Y. Epitope Mapping by HDX-MS Elucidates the Surface Coverage of Antigens Associated with High Blocking Efficiency of Antibodies to Birch Pollen Allergen. *Anal. Chem.* **2018**, *90* (19), 11315–11323.
- (50) Fang, M.; Wang, Z.; Cupp-Sutton, K. A.; Welborn, T.; Smith, K.; Wu, S. High-throughput hydrogen deuterium exchange mass spectrometry (HDX-MS) coupled with subzero-temperature ultrahigh pressure liquid chromatography (UPLC) separation for complex sample analysis. *Anal. Chim. Acta* **2021**, *1143*, 65–72.
- (51) Gu, T. Y.; Gu, Y.; Zheng, Y. Z. Phase-Separation of Acetonitrile-Water Mixture in Protein-Purification. *Sep. Technol.* **1994**, *4* (4), 258–260.
- (52) Zhang, L.; Shen, D.; Zhang, Z.; Wu, X. Experimental Measurement and Modeling of Vapor–Liquid Equilibrium for the Ternary System Water + Acetonitrile + Ethylene Glycol. *J. Chem. Eng. Data* **2017**, *62* (5), 1725–1731.
- (53) Guttman, M.; Lee, K. K. Chapter Fifteen - Isotope Labeling of Biomolecules: Structural Analysis of Viruses by HDX-MS. In *Methods in Enzymology*, Kelman, Z., Ed.; Vol. 566; Academic Press, 2016; pp 405–426.
- (54) Fang, J.; Rand, K. D.; Beuning, P. J.; Engen, J. R. False EX1 signatures caused by sample carryover during HX MS analyses. *Int. J. Mass Spectrom.* **2011**, *302* (1–3), 19–25.
- (55) Hamuro, Y.; Coales, S. J. Optimization of Feasibility Stage for Hydrogen/Deuterium Exchange Mass Spectrometry. *J. Am. Soc. Mass Spectrom.* **2018**, *29* (3), 623–629.
- (56) JGCM 200 2012 International vocabulary of metrology – Basic and general concepts and associated terms (VIM) Joint Committee for Guides in Metrology 2012, 2008 ed. with minor corrections; Bureau International des Poids et Mesures, 2012.
- (57) Hudgens, J. W. Construction of a Dual Protease Column, Subzero (–30 °C) Chromatography System and Multi-channel Precision Temperature Controller for Hydrogen-Deuterium Exchange Mass Spectrometry. *J. Res. Natl. Bur. Stand. (U. S.)* **2020**, *125*, 125025.
- (58) Churchill, S. W.; Bernstein, M. A. Correlating Equation for Forced Convection From Gases and Liquids to a Circular Cylinder in Crossflow. *Journal of Heat Transfer* **1977**, *99* (2), 300–306.
- (59) Broeckhoven, K.; Desmet, G. Considerations for the use of ultra-high pressures in liquid chromatography for 2.1mm inner diameter columns. *J. Chromatogr. A* **2017**, *1523*, 183–192.
- (60) de Villiers, A.; Lauer, H.; Szucs, R.; Goodall, S.; Sandra, P. Influence of frictional heating on temperature gradients in ultra-high-pressure liquid chromatography on 2.1mm I.D. columns. *J. Chromatogr. A* **2006**, *1113* (1), 84–91.
- (61) Trabjerg, E.; Jakobsen, R. U.; Mysling, S.; Christensen, S.; Jørgensen, T. J. D.; Rand, K. D. Conformational Analysis of Large and Highly Disulfide-Stabilized Proteins by Integrating Online Electrochemical Reduction into an Optimized H/D Exchange Mass Spectrometry Workflow. *Anal. Chem.* **2015**, *87* (17), 8880–8888.

- (62) Krenkova, J.; Szekrenyes, A.; Keresztessy, Z.; Foret, F.; Guttman, A. Oriented immobilization of peptide-N-glycosidase F on a monolithic support for glycosylation analysis. *J. Chromatogr. A* **2013**, *1322*, 54–61.
- (63) Guo, R. R.; Comamala, G.; Yang, H. H.; Gramlich, M.; Du, Y. M.; Wang, T.; Zeck, A.; Rand, K. D.; Liu, L.; Voglmeir, J. Discovery of Highly Active Recombinant PNGase H(+) Variants Through the Rational Exploration of Unstudied Acidobacterial Genomes. *Front. Bioeng. Biotechnol.* **2020**, *8*. DOI: 10.3389/fbioe.2020.00741
- (64) Comamala, G.; Krogh, C. C.; Nielsen, V. S.; Kutter, J. P.; Voglmeir, J.; Rand, K. D. Hydrogen/Deuterium Exchange Mass Spectrometry with Integrated Electrochemical Reduction and Microchip-Enabled Deglycosylation for Epitope Mapping of Heavily Glycosylated and Disulfide-Bonded Proteins. *Anal. Chem.* **2021**, *93*, 16330.
- (65) Burns, K. M.; Rey, M.; Baker, C. A. H.; Schriemer, D. C. Platform Dependencies in Bottom-up Hydrogen/Deuterium Exchange Mass Spectrometry. *Mol. Cell. Biochem.* **2013**, *12* (2), 539–548.
- (66) Pascal, B. D.; Willis, S.; Lauer, J. L.; Landgraf, R. R.; West, G. M.; Marciano, D.; Novick, S.; Goswami, D.; Chalmers, M. J.; Griffin, P. R. HDX Workbench: Software for the Analysis of H/D Exchange MS Data. *J. Am. Soc. Mass Spectrom.* **2012**, *23* (9), 1512–1521.
- (67) Connelly, G. P.; Bai, Y.; Jeng, M.-F.; Englander, S. W. Isotope effects in peptide group hydrogen exchange. *Proteins: Struct., Funct., Bioinf.* **1993**, *17* (1), 87–92.
- (68) Henry, G. D.; Sykes, B. D. Determination of the rotational dynamics and pH dependence of the hydrogen exchange rates of the arginine guanidino group using NMR spectroscopy. *Journal of Biomolecular NMR* **1995**, *6* (1), 59–66.
- (69) Coales, S. J.; Tomasso, J. C.; Hamuro, Y. Effects of electrospray capillary temperature on amide hydrogen exchange. *Rapid Commun. Mass Spectrom.* **2008**, *22* (9), 1367–1371.
- (70) Woodward, C. K.; Ellis, L. M.; Rosenberg, A. The solvent dependence of hydrogen exchange kinetics of folded proteins. *J. Biol. Chem.* **1975**, *250* (2), 440–444.
- (71) Martin, M.; Guiochon, G. Effects of high pressure in liquid chromatography. *J. Chromatogr. A* **2005**, *1090* (1), 16–38.
- (72) Gritti, F.; Guiochon, G. Optimization of the thermal environment of columns packed with very fine particles. *J. Chromatogr. A* **2009**, *1216* (9), 1353–1362.
- (73) De Vos, J.; Broeckhoven, K.; Eeltink, S. Advances in Ultrahigh-Pressure Liquid Chromatography Technology and System Design. *Anal. Chem.* **2016**, *88* (1), 262–278.
- (74) Kaplitz, A. S.; Kresge, G. A.; Selover, B.; Horvat, L.; Franklin, E. G.; Godinho, J. M.; Grinias, K. M.; Foster, S. W.; Davis, J. J.; Grinias, J. P. High-Throughput and Ultrafast Liquid Chromatography. *Anal. Chem.* **2020**, *92* (1), 67–84.
- (75) Del Mar, C.; Greenbaum Eric, A.; Mayne, L.; Englander, S. W.; Woods Virgil, L. Structure and properties of α -synuclein and other amyloids determined at the amino acid level. *Proc. Natl. Acad. Sci. U. S. A.* **2005**, *102* (43), 15477–15482.
- (76) Mayne, L.; Kan, Z. Y.; Chetty, P. S.; Ricciuti, A.; Walters, B. T.; Englander, S. W. Many Overlapping Peptides for Protein Hydrogen Exchange Experiments by the Fragment Separation-Mass Spectrometry Method. *J. Am. Soc. Mass Spectrom.* **2011**, *22* (11), 1898–1905.
- (77) Fajer, P. G.; Bou-Assaf, G. M.; Marshall, A. G. Improved Sequence Resolution by Global Analysis of Overlapped Peptides in Hydrogen/Deuterium Exchange Mass Spectrometry. *J. Am. Soc. Mass Spectrom.* **2012**, *23* (7), 1202–1208.

Recommended by ACS

Simple Platform for Automating Decoupled LC–MS Analysis of Hydrogen/Deuterium Exchange Samples

Michael J. Watson, Miklos Guttman, *et al.*

DECEMBER 07, 2020
JOURNAL OF THE AMERICAN SOCIETY FOR MASS SPECTROMETRY

READ 

Improving Spectral Validation Rates in Hydrogen–Deuterium Exchange Data Analysis

Shaunak Raval, David C. Schriemer, *et al.*

FEBRUARY 16, 2021
ANALYTICAL CHEMISTRY

READ 

Characterization and Management of Noise in HDX-MS Data Modeling

Ramin Ekhteiri Salmas and Antoni James Borysik

MAY 07, 2021
ANALYTICAL CHEMISTRY

READ 

Enhanced Sequence Coverage of Large Proteins by Combining Ultraviolet Photodissociation with Proton Transfer Reactions

James D. Sanders, Jennifer S. Brodbelt, *et al.*

NOVEMBER 26, 2019
ANALYTICAL CHEMISTRY

READ 

Get More Suggestions >